# Quartz Enhanced Photoacoustic sensors for detection of multiple hydrocarbon and methane isotopes

Giansergio Menduni[a,b], Angelo Sampaolo[a], Sebastian Csutak[c], Pietro Patimisco[a], Marilena Giglio[a], Arianna Elefante[a], Vittorio Passaro[b], Frank K. Tittel[d], Max Deffenbaugh[c] and Vincenzo Spagnolo[a]

[a] PolySense Lab - Dipartimento Interateneo di Fisica, University and Politecnico of Bari, Via Amendola 173, Bari, Italy
[b]Photonics Research Group, Dipartimento di Ingegneria Elettrica e dell'informazione, Politecnico di Bari, Via Orabona 4, Bari, 70126, Italy
[c] Aramco Service Company, 16300 Park Row Dr, Houston TX, 77084
[d]Department of Electrical and Computer Engineering, Rice University, 6100 Main Street, Houston, TX 77005, USA

## ABSTRACT

Hydrocarbon detection in the gas phase can be a powerful tool to guide downstream operations for the oil & gas industry. This application requires highly sensitive, selective and robust spectroscopic techniques. In this work we present: i) a quartz-enhanced photoacoustic (QEPAS) sensor that can individually detect methane and ethane in the part-per billion range and propane in the ppm range by employing a single interband cascade laser emitting at 3345 nm; ii) a QEPAS sensor detecting $^{12}CH_4$ and $^{13}CH_4$ isotopes at the part-per billion sensitivity level, by employing a quantum cascade laser emitting at 7730 nm.

**Keywords:** quartz-enhanced photoacoustic spectroscopy, gas sensing, hydrocarbons, quartz tuning fork, isotopes.

## 1. INTRODUCTION

In the oil&gas field all the down-, mid- and up-stream operations aim to optimize the costs by empowering the exploration phase with valuable tools devoted to analysis for the estimation of reservoirs as well as the evaluation of the quality of the rocks. In this perspective, the detection of hydrocarbons in the gas phase provides a robust and reliable asset for guiding exploration and drilling, avoiding dry holes and increasing the forecasting efficiency. Therefore, the next big step to be taken for trace gas sensors is the detection and monitoring of biomarkers and related isotopic ratios in natural gas samples, instead of nitrogen-diluted mixtures usually available in research laboratories. One of the most selective and sensitive approaches to detect hydrocarbons in the gas phase is the employment of laser based spectroscopic techniques [1-4]. The main challenges in the design and realization of effective and reliable sensors are: i) identification of spectral signatures that univocally characterize a specific hydrocarbon in a natural gas mixture; ii) identification of the optimum working conditions in order to distinguish absorption features related to different isotopes of the same hydrocarbon; iii) engineering of the experimental apparatus to facilitate the integration into pre-existing tools devoted to the analysis and characterization of the drilling products. Among different optical techniques for trace gas analysis, quartz-enhanced photoacoustic spectroscopic (QEPAS) stands out because it can offer robustness and compactness without affecting sensitivity and selectivity [5-15] In this work, we present two QEPAS sensors: the first one based on a standard quartz tuning fork (QTF) and an interband cascade laser (ICL) to determine the natural gas composition [16], and the second one employing a custom QTF and a quantum cascade laser (QCL) for monitoring the methane 13C/12C isotopic ratio. The architecture of the first sensor is designed for in-situ and real time detection. The second sensor is still at the prototype stage but it shows all the potentialities to be integrated in self-consistent sensor able to analyze the natural gas composition and isotopic ratio in order to determine the bio- or thermogenic origin of the crude oil [16,17].

Quantum Sensing and Nano Electronics and Photonics XVI, edited by Manijeh Razeghi, Proc. of SPIE
Vol. 10926, 109260C · © 2019 SPIE · CCC code: 0277-786X/19/$18 · doi: 10.1117/12.2507881

## 2. SENSOR ARCHITECTURE FOR METHANE, ETHANE AND PROPANE DETECTION

The infrared spectral region that we identified for detecting methane ($CH_4$ or C1), ethane ($C_2H_6$ or C2) and propane ($C_3H_8$ or C3) is the 2986-2990 $cm^{-1}$ window [18-19]. The ICL laser source (Nanoplus) and its central emission wavelength at 3345 nm was chosen in order to exploit absorption features related to C1 and C2 with the strongest cross-sections [19]. The ICL tuning range covers also C3 broadband absorption features. By keeping fixed the ICL temperature at 15°C and spanning the laser current from 20 mA up to 70 mA, it was possible to target a threefold C1 absorption structure with the strongest line peaked at 2988.8 $cm^{-1}$ ($\upsilon_3^{C1}$), and two C2 lines located at 2990.1 $cm^{-1}$ ($\upsilon_1^{C2}$) and 2986.25 $cm^{-1}$ ($\upsilon_2^{C2}$), respectively. In Ref [18], the experimental apparatus and the optimized conditions for detecting C1 and C2 in a laboratory working environment, at low pressures and with sensitivity levels in the ppb scale are described in detail. In this manuscript, we will discuss how starting from a benchtop prototype apparatus we developed a robust compact sensor suitable for deployment at the well site.


Figure 1. Front and rear panel of the shoebox sized hydrocarbon sensor.

Fig. 1 shows the front and rear panel of the developed quartz enhanced photoacoustic spectrometer for C1, C2, C3 detection. Compared to the original configuration of the bench top prototype, this configuration is more versatile and simpler. In fact, instead of working with a continuous gas flow at 200 Torr, it works in a static regime at the atmospheric pressure. This allowed to replace the pressure controller with a simpler pressure meter. If the gas sample is at atmospheric pressure, an external pump allows the gas flowing through the acoustic detection module (ADM), while for overpressure samples the gas mixture freely fluxes through the sensor. The overall size of the case is 30 cm × 10 cm × 20 cm. Inside the box the optical components, the ICL, the ADM, the gas line, the pressure meter and a power meter for alignment purposes are installed. The ADM is composed by a standard 32 kHz QTF equipped with a dual tube micro-resonator system for sound wave amplification. A NI-DAQ board modulates the ICL and acquires the QTF signal. A LabVIEW-based software was used to handle the current driver/temperature controller (Thorlabs ITC4002QCL), the pressure meter, the power meter. A dedicated sub-routine of the software acts as a lock-in detector for the QEPAS signal demodulation at different integration times.

## 3. MEASUREMENT FLOW CHART AND DATA ANALYSIS

The operations managed by the software can be divided into three macro-sequences: i) electrical characterization of the resonator for the determination of the QTF's characteristic parameters such as the frequency and quality factor [20-22]; ii) current scan in the wavelength range containing the selected spectral features of C1, C2, C3; iii) analysis of the QEPAS signal for the determination of the hydrocarbon concentrations. In the first sequence, after the mixture reached the atmospheric pressure inside the ADM, the software commands the NI-DAQ to generate a sinusoidal voltage signal to excite the QTF. The excitation frequency is swept around the expected resonance frequency of the QTF. The frequency sweep resolution was 0.1 Hz. The QTF's response to the electrical excitation is demodulated at the same modulation frequency and the obtained resonance curve is fitted with a Voigt profile [23-24]. This provides the peak frequency $f_0$, the full width half-maximum of the resonance curve and the related quality factor $Q$. In the second sequence, a current saw-tooth ramp is fed to laser together with a fast sinusoidal modulation at $f_0/2$ frequency. The optimized modulation depth was 300 mVp-p. The frequency of the saw-tooth ramp ranges from 2 mHz to 30 mHz. The QEPAS voltage signal

is acquired step by step and instantly demodulated at the resonance frequency of the QTF by means of the LabVIEW lock-in subroutine. In the third phase, the QEPAS signal is fitted by a linear combination of reference spectra.

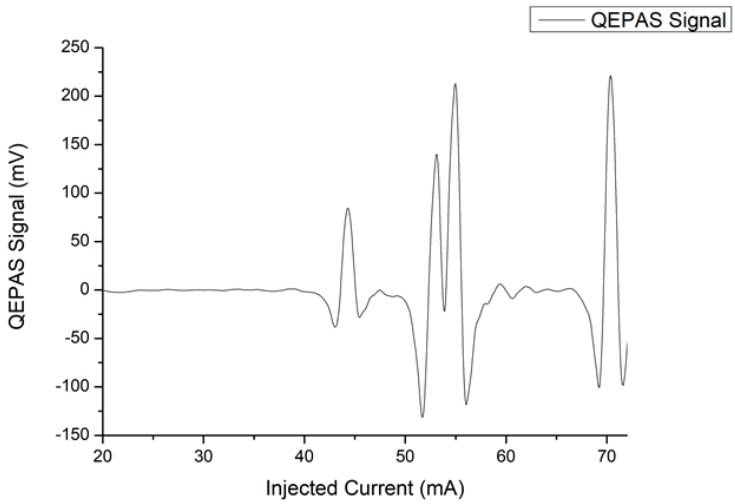


Figure 2. QEPAS signal acquired for a natural gas-like sample.

The reference spectra used by the fitting subroutine are the QEPAS signals acquired for mixtures of C1-1000 ppm:$N_2$, C2-1000 ppm:$N_2$ and C3-1000ppm:$N_2$ respectively. The reference spectra were acquired at a fixed detection phase. The product between the reference concentration (1000 ppm) and the coefficients obtained from the linear combination fitting the QEPAS spectrum of the mixture provides the effective concentration for each hydrocarbon. In Fig. 2, is shown the QEPAS signal acquired for a gas sample obtained by diluting a natural gas sample (C1-85%, C2-5%, C3-3%, C4 2%, $CO_2$ 2%, $N_2$- 3%) at 10% in pure $N_2$. The natural gas sample concentrations retrieved from the fit were C1 85±3%, C2 5±0.4 %, C3 3±0.8 %. In Ref. [18], we demonstrated that the detection limits achievable for C1, C2 are respectively 90 ppb and 7 ppb at 1 second of integration time [15]. For C3 increases to 3 ppm. Thus, although the minimum detection sensitivities are in the ppm or sub ppm scale, the developed sensor is able to measure hydrocarbon concentrations that can reach 90%, like methane in a typical composition of natural gas.

## 4. $^{12}CH_4$ $^{13}CH_4$ ISOTOPES DETECTION

In addition to the natural gas composition, it is also important to determine the hydrocarbon isotopic ratios. To address this issue, a prototype QEPAS sensor capable to selectively determine $^{12}CH_4$ (C12) and $^{13}CH_4$ (C13) concentration were demonstrated. The QEPAS sensor employed a distributed feedback quantum cascade laser emitting at 7.73 µm as optical excitation source and an ADM mounting a custom T-shaped QTF as optoacoustic detector. Apart from the laser and the QTF, the experimental apparatus configuration is identical to the benchtop prototype described in the Ref. [18]. Nevertheless, for $^{12}CH_4$ and $^{13}CH_4$ isotope detection is necessary to target transitions related to the C-H bond bending, located in the 7.3 µm – 7.8 µm range. In this range, the two isotopes show pairs of absorption features with comparable cross-sections. Since the beam waist dimensions for QCL emitting in the range of interest are larger than those at 3.3 µm, a QTF with innovative geometry has been exploited.

.

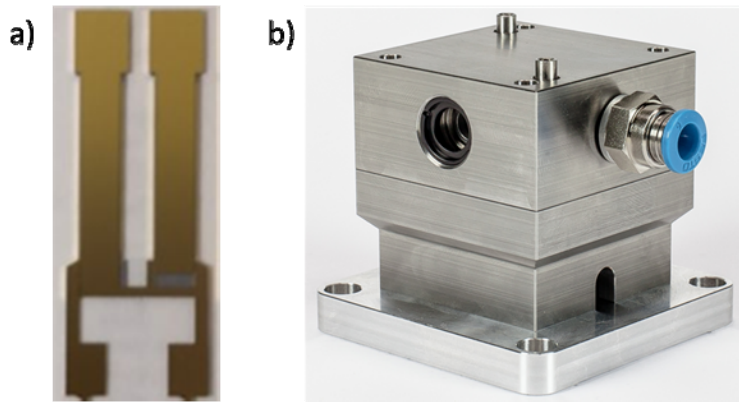


Figure 3. (a) Picture of a custom T-shaped QTF resonating at ~ 12 kHz b) custom acoustic detection module accommodating the T-shaped QTF and the micro-resonator tubes.

In Fig. 3(a) a picture of the employed custom QTF [25-33] is shown. The T-shaped QTF was mounted in a custom ADM (Fig. 3b)), built specifically for accommodating the QTF and two micro-resonator tubes in on-beam configuration, having a total length of 20 mm. The ADM is also equipped with a custom low noise preamplifier. The T-shaped QTF operates at frequency ~ 12 kHz (more than half of the standard 32 kHz QTF) and is more suited to detect gas with low relaxation rates such as methane. The micro-resonator tubes guarantee a signal to noise enhancement of ~ ×40. For methane isotopes detection two lines falling at 1296.12 $cm^{-1}$ for $^{12}CH_4$ and 1296.03 $cm^{-1}$ for $^{13}CH_4$ have been selected. In the lower panel of Fig. 4 are the two features cross-sections at 50 Torr, as provided by HITRAN database [19]. The absorption cross-section takes into account the natural abundance of each isotope (~ 98.82% $^{12}CH_4$, 1.11% $^{13}CH_4$). The cross-section ratio is $\sigma_{13}/\sigma_{12}$ ~ 0.06. The most important requirement is to operate at a pressure suitable for separating the QEPAS signals belonging to the two absorption lines. The optimal operating pressure, also in terms of QEPAS signal, was 50 Torr.

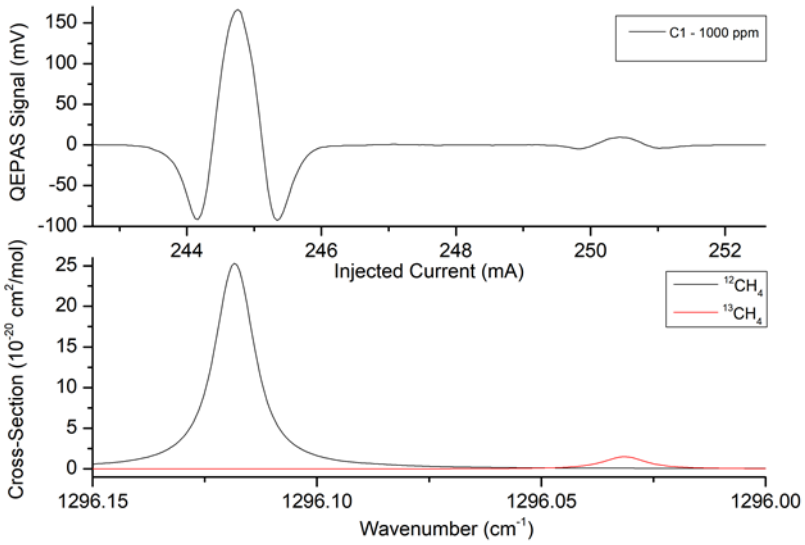


Figure 4. (a) Lower panel: absorption cross-section for the $^{12}CH_4$ (black line) and $^{13}CH_4$ (red line) absorption features at 50 Torr; upper panel: 2f-QEPAS signal recorded for methane at 1000 ppm in pure $N_2$ at a pressure of 50 Torr. The QCL injected current scan in the upper panel corresponds to the wavelength tuning reported in the lower panel 1296 - 1296.15 $cm^{-1}$.

In Fig.4 (upper panel) is shown the QEPAS spectrum acquired for a mixture of 1000 ppm of standard methane in $N_2$ at 50 Torr. The 242.6 mA – 252.6 mA QCL injected current scan corresponds to a wavelength tuning from 1296 $cm^{-1}$ – 1296.15 $cm^{-1}$. The modulation depth was set 7.5 $mV_{p-p}$. As can be seen from the upper panel of Fig. 4, the two features related to the isotope C12 and C13 are perfectly distinguishable. The ratio between the related QEPAS peak signals $S_{13}/S_{12}$ is ~ 0.06. We further diluted in $N_2$ the certified mixture down to 50 ppm of standard methane verifying a perfect linearity for the 2f-QEPAS signal peaks of both isotope 12 and 13. For all the concentrations it was always found the same ratio $S_{13}/S_{12}$ ~ 0.06, in perfect agreement with the related cross-section ratio. The standard deviation of the noise level is 0.1 mV, while the $^{13}CH_4$-QEPAS signal peak for a concentration of 11 ppm resulted ~ 10 mV. This corresponds to a minimum detection limit of 115 ppb achievable at 0.1 s of lock-in integration time. In the same way, the $^{12}CH_4$ minimum detection limits at the same operating conditions was 600 ppb.

## 5. CONCLUSIONS

In this manuscript, we have reported on the realization of a compact and robust QEPAS sensor ready to be deployed at the well site. At the same time, we also reported on the demonstration of a prototype QEPAS sensor able to detect $^{12}CH_4$ and $^{13}CH_4$ isotope, with detection limits of 600 ppb and 115 ppb at 0.1 sec integration time, respectively. The final goal will be the integration of methane isotope QEPAS sensor into a full system to be deployed at the well sites for measurement of main hydrocarbon composition and isotopic ratio of methane in natural gas mixtures.
.

## 6. AKNOWLEDGMENTS

The authors from Dipartimento Interateneo di Fisica di Bari acknowledge financial support from THORLABS GmbH, within the joint research laboratory PolySense. Frank K. Tittel acknowledges support by the Welch Foundation under Grant No. C0568.

## REFERENCES

[1] Liu X., Cheng S., Liu H., Hu S., Zhang D., Ning H., "A Survey on Gas Sensing Technology," Sensors 12, 9635–9665 (2012).
[2] Hodgkinson, J., and Tatam, R.P., "Optical gas sensing: A review," Meas. Sci. Technol. 24, 012004 (2013).
[3] Galli I., Bartalini S., Borri S., Cancio P., Mazzotti D., De Natale P., Giusfredi G., "Molecular Gas Sensing Below Parts Per Trillion: Radiocarbon-Dioxide Optical Detection," Phys. Rev. Lett., 107, 270802:1-270802:4 (2011).
[4] Patimisco, P., Sampaolo, A., Dong, L., Tittel, F.K., Spagnolo V., "Recent advances in quartz enhanced photoacoustic sensing," Appl. Phys. Rev., 011106 (2018).
[5] Patimisco, P., Scamarcio, G., Tittel, F.K., Spagnolo, V., "Quartz-Enhanced Photoacoustic Spectroscopy: A Review," Sensors 14, 6165-6206 (2014).
[6] Patimisco, P., Sampaolo, A., Zheng, H., Dong, L., Tittel, F.K. and Spagnolo V., "Quartz enhanced photoacoustic spectrophones exploiting custom tuning forks: a review," Adv. Phys. X 2, 169-187 (2016).
[7] Patimisco, P., Sampaolo, A., Dong, L., Tittel, F.K., Spagnolo V., "Recent advances in quartz enhanced photoacoustic sensing," Appl. Phys. Rev., 011106 (2018).
[8] Jahjah, M., Jiang, W., Sanchez, N.P., Ren, W., Patimisco, P., Spagnolo, V., Herndon, S.C., Griffin, R.J., and Tittel, F.K., "Atmospheric $CH_4$ and $N_2O$ measurements near Greater Houston area landfills using QCL-based QEPAS sensor system during DISCOVERY-AQ 2013," Opt. Lett. 39, 957-960 (2014).
[9] Sampaolo, A., Patimisco, P., Giglio, M., Chieco, L., Scamarcio, G., Tittel, F.K., and Spagnolo, V., "Highly sensitive gas leak detector based on a quartz-enhanced photoacoustic $SF_6$ sensor," Opt. Express 24, 15872-15881 (2016).
[10] Patimisco, P., Spagnolo, V., Vitiello, M. S., Tredicucci, A., Scamarcio, G., Bledt, C. M., and Harrington, J. A., "Coupling external cavity mid-IR quantum cascade lasers with low loss hollow metallic/dielectric waveguides," Appl. Phys. B 108, 255–260 (2012).

[11] Viciani, S., Siciliani de Cumis, M., Borri, S., Patimisco, P., Sampaolo, A., Scamarcio, G., De Natale, P., D'Amato, F., and Spagnolo, V., "A quartz-enhanced photoacoustic sensor for H2S trace-gas detection at 2.6 μm," Appl. Phys. B 119, 21-27 (2014).
[12] Giglio, M., Patimisco, P., Sampaolo, A., Zifarelli, A., Blanchard, R., Pfluegl, C., Witinski, M.F., Vakhshoori, D., Tittel, F.K., and Spagnolo, V., Nitrous oxide quartz-enhanced photoacoustic detection employing a broadband distributed-feedback quantum cascade laser array," Appl. Phys. Lett. 113, 171101 (2018).
[13] Patimisco, P., Sampaolo, A., Giglio, M., Mackoviak, V., Rossmadl, H., Gross, B., Cable, A., Tittel, F.K., and Spagnolo, V., "Octupole electrode pattern for tuning forks vibrating at the first overtone mode in quartz-enhanced photoacoustic spectroscopy," Opt. Lett. 43, 1854-1857 (2018).
[14] Dong, L., Kosterev, A.A., Thomazy, D., Tittel, F.K., "QEPAS spectrophones: design, optimization, and performance," Appl. Phys. B 100, 627–635 (2010).
[15] Giglio, M., Patimisco, P., Sampaolo, A., Scamarcio, G., Tittel, F. K., and Spagnolo, V., "Allan Deviation Plot as a Tool for Quartz-Enhanced Photoacoustic Sensors Noise Analysis," IEEE Trans. Ultrason. Ferroelect. Freq. Control 63, 555-560 (2016).
[16] Webster, C.R., "Measuring methane and its isotopes $^{12}CH_4$, $^{13}CH_4$, and $CH_3D$ on the surface of Mars with in situ laser spectroscopy," Appl. Optics 44, 1226-1235 (2005).
[17] Yamamoto, K., and N. Yoshida. "High-precision isotopic ratio measurement system for methane ($^{12}CH_3D/^{12}CH_4$, $^{13}CH_4/^{12}CH_4$) by using near-infrared diode laser absorption spectroscopy." Spectrochim. Acta A 58, 2699-2707 (2002).
[18] Sampaolo A., Csutak S., Patimisco P., Giglio M., Menduni G., Passaro V., Tittel F.K., Deffenbaugh M., and Spagnolo V., "Methane, ethane and propane detection using a compact quartz enhanced photoacoustic sensors and a single interband cascade laser", Sens. Act. B Chem. 282, 952-960 (2019).
[19] www.hitran.com
[20] Patimisco, P., Sampaolo, A., Dong, L., Giglio, M., Scamarcio, G., Tittel, F.K., and Spagnolo, V., "Analysis of the electro-elastic properties of custom quartz tuning forks for optoacoustic gas sensing," Sensor Actuat. B-Chem. 227, 539-546 (2016).
[21] Patimisco, P., Borri, S., Sampaolo, A., Beere, H.E., Ritchie, D.A., Vitiello, M.S., Scamarcio, G., and Spagnolo, V., "Quartz enhanced photo-acoustic gas sensor based on custom tuning fork and terahertz quantum cascade laser," Analyst 139, 2079-2087 (2014).
[22] Patimisco, P., Sampaolo, A., Mackowiak, V., Rossmadl, H., Cable, A., Tittel, F.K., and Spagnolo, V., "Loss Mechanisms Determining the Quality Factors in Quartz Tuning Forks Vibrating at the Fundamental and First Overtone Modes," IEEE Trans. Ultrason. Ferroelect. Freq. Control 65, 1951-1957 (2018).
[23] Bidaux, Y., Bismuto, A., Patimisco, P., Sampaolo, A., Gresch, T., Strubi, G., Blaser, S., Tittel, F.K., Spagnolo, V., Muller, A., and Faist, J., "Mid infrared quantum cascade laser operating in pure amplitude modulation for background-free trace gas spectroscopy," Opt. Express 24, 26464-26471 (2016).
[24] Patimisco, P., Sampaolo, A., Bidaux, Y., Bismuto, A., Schott, M., Jiang, J., Muller, A., Faist, J., Tittel, F.K., and Spagnolo, V., "Purely wavelength- and amplitude-modulated quartz-enhanced photoacoustic spectroscopy," Opt. Express 24, 25943-25954 (2016).
[25] Wu, H., Sampaolo, A., Dong, L., Patimisco, P., Liu, X., Zheng, H., Yin, X., Ma, W., Zhang, L., Yin, W., Spagnolo, V., Jia, S., and Tittel, F.K., "Quartz enhanced photoacoustic $H_2S$ gas sensor based on a fiber-amplifier source and a custom tuning fork with large prong spacing," Appl. Phys. Lett. 107, 111104 (2015).
[26] Sampaolo, A., Patimisco, P., Giglio, M., Vitiello, M.S., Beere, H.E., Ritchie. D.A., Scamarcio, G., Tittel, F. K., and Spagnolo, V., "Improved Tuning Fork for Terahertz Quartz-Enhanced Photoacoustic Spectroscopy," Sensors, 16, 439 (2016).
[27] Spagnolo, V., Patimisco, P., Pennetta, R., Sampaolo, A., Scamarcio, G., Vitiello, M.S., Tittel, F.K., "THz Quartz-enhanced photoacoustic sensor for $H_2S$ trace gas detection," Opt. Express 23, 7574-7582 (2015).
[28] Sampaolo, A., Patimisco, P., Dong, L., Geras, A., Scamarcio, G., Starecki, T., Tittel, F. K., and Spagnolo, V., "Quartz-enhanced photoacoustic spectroscopy exploiting tuning fork overtone modes," Appl. Phys. Lett. 107, 231102 (2015).
[29] Zheng, H., Dong, L., Sampaolo, A., Wu, H., Patimisco, P., Yin, X., Ma, W., Zhang, L., Yin, W., Spagnolo, V., Jia, S., Tittel, F.K., "Single-tube on-beam quartz-enhanced photoacoustic spectroscopy," Opt. Lett. 41, 978-981 (2016).

[30] Zheng, H., Dong, L., Patimisco, P., Wu, H., Sampaolo, A., Yin, X., Li, S., Ma, W., Zhang, L., Yin, W., Xiao, L., Spagnolo, V., Jia, S., Tittel, F.K., "Double antinode excited quartz-enhanced photoacoustic spectrophone," Appl. Phys. Lett. 110, 021110 (2017).
[31] Wu, H., Yin, X., Dong, L., Pei, K., Sampaolo, A., Patimisco, P., Zheng, H., Ma, W., Zhang, L., Yin, W., Xiao, L., Spagnolo, V., Jia, S., Tittel, F.K., "Simultaneous dual-gas QEPAS detection based on a fundamental and overtone combined vibration of quartz tuning fork," Appl. Phys. Lett. 110, 121104 (2017).
[32] Zheng, H., Dong, L., Sampaolo, A., Wu, H., Patimisco, P., Ma, W., Zhang, L., Yin, W., Xiao, L., Spagnolo, V., Jia, S., and Tittel, F.K., "Overtone resonance enhanced single-tube on-beam quartz enhanced photoacoustic spectrophone," Appl. Phys. Lett. 109, 111103 (2016).
[33] Tittel, F.K., Sampaolo, A., Patimisco, P., Dong, L., Geras, A., Starecki, T., and Spagnolo, V., "Analysis of overtone flexural modes operation in quartz-enhanced photoacoustic spectroscopy," Opt. Express 24, A682-A692 (2016).